9

Research article

Baiwei Mao, Yange Liu*, Hongwei Zhang, Kang Yang, Ya Han, Zhi Wang and Zhaohui Li

Complex analysis between CV modes and OAM modes in fiber systems

https://doi.org/10.1515/nanoph-2018-0179
Received October 23, 2018; revised December 3, 2018; accepted December 4, 2018

Abstract: As two groups of bases in fibers, cylindrical vector (CV) modes and the orbital angular momentum (OAM) modes can be transformed into each other. Several transformation relations have been studied in previous works, such as $\hat{\sigma}^+$ **0AM**_{+l} = $HE_{l+1,m}^{\text{even}} + iHE_{l+1,m}^{\text{odd}}$. However, these relations are discussed in the limitation of equal amplitude, limited phase difference $\left(\frac{k\pi}{2}, k \in Z\right)$ and finite (generally two) mode bases. Complete connection between the CV and OAM modes has not been found. In this paper, a four-dimensional complex space model is constructed to describe arbitrary CV and OAM modes. The reliability of the model is verified by previously reported results and our experiment results. The complete transformation relation between the CV modes and OAM modes is well described in the model. Furthermore, two common kinds of relations have been researched, that is, a single arbitrary polarized OAM mode and two arbitrary orthogonal polarized OAM modes and their corresponding CV modes. These two kinds of states include most of previously reported states, and some new states have not been reported.

Keywords: cylindrical vector mode; orbital angular momentum mode; fiber optics; mode transformation; complex analysis.

Baiwei Mao, Hongwei Zhang, Kang Yang, Ya Han and Zhi Wang: Tianjin Key Laboratory of Optoelectronic Sensor and Sensing Network Technology, and Institute of Modern Optics, Nankai University, Tianjin 300071, P.R. China

Zhaohui Li: State Key Lab Optoelectric Material and Technology, School of Electric and Information Technology, Sun Yat Sen University, Guangzhou 510275, P.R. China

1 Introduction

Cylindrical vector (CV) modes, as a group of intrinsic bases in fibers, have been studied for a long time [1]. As the eigensolutions of Helmholtz equation in ideal fiber, CV modes are the intrinsic states that can be propagated stably in fibers. Any electric field in fibers can be presented in the bases of CV modes. CV modes are divided into different orders. In each order, there are four degenerated CV modes, whose propagation constants are almost the same. For the *l*th (l>0) order modes, they consist of four degenerated modes, named $EH^{\mathrm{even}}_{l-1,m}, EH^{\mathrm{odd}}_{l-1,m}, HE^{\mathrm{even}}_{l+1,m}, HE^{\mathrm{odd}}_{l+1,m}$ for l>1 and $TM_{0,m}$, $TE_{0,m}$, $HE_{2,m}^{\mathrm{even}}$, $HE_{2,m}^{\mathrm{odd}}$ for l=1, also named higherorder modes. The 0th order modes are combined by two degenerated modes, named HE_{11}^{even} and HE_{11}^{odd} , also named fundamental modes. l is the azimuthal order and m is the radial order of CV modes. In principle, l and m can take any integer number from 0 to $+\infty$. Generally, the radial order m is not important, so we will just discuss the azimuthal order l. There is a singular area in the center of the pattern of lth (l>0) order modes where the intensity vanishes. This is because the radial intensity is determined by an Ith-order Bessel function for step index fibers (or other functions with similar properties for other axisymmetric index profile fibers), which is zero at the center when l > 0. Moreover, the polarization states of CV modes are spatially inhomogeneous. That is, for different points on the beam cross-section of CV modes, the polarization states vary from their azimuthal angles. These properties are unique compared with conventional light waves. It leads to some potential applications in optical manipulation [2-5], highresolution microscopy [6], optical communication [7–11], and data storage [12].

Orbital angular momentum (OAM) modes, as another group of bases found almost three decades ago [13], are attracting more and more attention in recent years [14–17]. OAM modes are characterized by a helical phase front $e^{\pm il\xi}$, where $\pm l$ is topological charge (TC) and ξ is the azimuthal angle related to the optic axis. l can take the integer numbers from 0 to $+\infty$. Notice that l is the same as the azimuthal order mentioned above, which will be discussed soon. In the beam cross-section, the polarization

^{*}Corresponding author: Yange Liu, Tianjin Key Laboratory of Optoelectronic Sensor and Sensing Network Technology, and Institute of Modern Optics, Nankai University, Tianjin 300071, P.R. China, e-mail: ygliu@nankai.edu.cn. https://orcid.org/0000-0003-3428-5692

(amplitude and direction of electric vector) of each point can arrive to that of another point with the same radius, but at a different time or propagation distance. In other words, for different points on the beam cross-section with the same radius, the polarization states are the same, but different in phase. This indicates the helical phase front of OAM modes. Due to its unique phase properties, OAM beams are becoming a useful tool in atom manipulation [18–20], nanoscale microscopy [21], optical tweezers [22–24], optical communication [25–29], and data storage

As two mode bases in fibers, there should be a transformation relation between OAM modes and CV modes. However, people just found some particular states linking OAM modes and CV modes. Han et al. [32] has reported circular OAM modes generated by combining even and odd modes of the first- and second-order CV modes, that is, $\hat{\sigma}^{\pm} OAM_{_{\pm 2}} = EH_{_{11}}^{even} \pm iEH_{_{11}}^{odd}$, $\hat{\sigma}^{\pm} OAM_{_{\pm 1}} = TM_{_{01}} \pm iTE_{_{01}}$ and $\hat{\sigma}^{\pm} OAM_{_{\pm 2}} = HE_{_{31}}^{even} \pm iHE_{_{31}}^{odd}$, $\hat{\sigma}^{\pm} OAM_{_{\pm 1}} = HE_{_{21}}^{even} \pm iHE_{_{21}}^{odd}$. $\hat{\sigma}^{\scriptscriptstyle +}(\hat{\sigma}^{\scriptscriptstyle -})$ represents the left-hand (right-hand) circular polarized direction. Jiang has reported the transformation relations of $\hat{x}OAM_{\pm 1} \pm i\hat{y}OAM_{\pm 1} = TE_{01} \mp iHE_{21}^{\text{even}}$, $\hat{x}OAM_{+1} \pm \hat{y}OAM_{\pm 1} = TM_{01} \pm iHE_{21}^{\text{odd}}$ in step index fiber [33] and ring-core fiber [34]. $\hat{x}(\hat{y})$ represents the polarized direction along the x(y)-axis. And they separate these hybrid states into two pure OAM modes by a polarizer. Han et al. [35] has reported the generation of OAM modes by TM_{ox} , TE_{01} , $TM_{01} + TE_{01}$, and $TM_{01} - TE_{01}$, which correspond to two circular orthogonal polarized OAM modes, also corresponding to the superposition of two orthogonal polarized linear polarized (LP) modes [36]. Wu et al. [37] has reported the connection of the first- and the second-order LP OAM $\begin{array}{l} \text{modes and LP modes, } \hat{x}(\hat{y}) \text{OAM}_{\pm 1} = \hat{x}(\hat{y}) L P_{11}^{\text{even}} \pm i \hat{x}(\hat{y}) L P_{11}^{\text{odd}}, \\ \hat{x}(\hat{y}) \text{OAM}_{\pm 2} = \hat{x}(\hat{y}) L P_{21}^{\text{even}} \pm i \hat{x}(\hat{y}) L P_{21}^{\text{odd}}. \quad \text{Previous} \quad \text{articles} \end{array}$ have demonstrated several combination states in which CV modes can be transformed into OAM modes. However, their selected combinations are too simple. In conclusion, they just select the complex amplitudes of CV modes as ± 1 or $\pm i$ (equal-amplitude and limited phase difference $\left(\frac{k\pi}{2}, k \in Z\right)$, and the CV modes used to generate OAM

modes are generally no more than two. That is not enough. In reality, to totally describe the *l*th-order electric field in fibers, we need combine the four degenerated CV modes in arbitrary amplitude and phase. This means we should not only consider the complex amplitudes of CV modes as arbitrary complex number but also consider the four degenerated CV modes simultaneously. Moreover, previous works just reveal the properties of circular or LP OAM modes. However, the most general elliptical polarized OAM modes have not been discussed in the past.

In this paper, we break the limitations of previous papers and derive the complete transformation relation of arbitrary Ith modes between CV modes and OAM modes in four-dimensional complex space. Through this transformation relation, for any combination of CV modes (OAM modes) in fibers, one can calculate the corresponding OAM modes (CV modes) equivalent to it. The reliability of the proposed four-dimensional complex space model is well verified by previous reports and our experiment results [32-45]. As will be shown soon, it is much more intuitive to analyze a specific kind of mode when the electric fields are expressed in the corresponding mode bases. If the OAM mode is to be analyzed, the mathematical expression of the field in OAM modes will be the simplest. For example, $EH_{l-1,m}^{\mathrm{even}} - iHE_{l+1,m}^{\mathrm{odd}}$, one may not be able to tell if this state can be used to generate OAM modes. However, when expressing the same electric field into OAM mode bases, we get $EH_{l-1,m}^{\mathrm{even}} - iHE_{l+1,m}^{\mathrm{odd}} = \hat{x}\mathrm{OAM}_{-l} + i\hat{y}\mathrm{OAM}_{+l}$. Now, one can recognize this state as the superposition of two orthogonal polarized OAM modes and can be separated by polarizer. Most previous articles present the mode field in fiber in CV mode bases, even studying the OAM modes. It is not intuitive to research the properties of OAM modes. To simplify the verification of our model for readers, we still give the electric field in CV mode bases and OAM mode bases simultaneously in Section 3, "Results and Discussion." Furthermore, in discussing the properties of OAM modes better, we sort the results into six situations and give the corresponding general formulas to describe each of them. The first four situations are enough to include most of reported works [32-45]. The last two situations are the extended states, which describe the elliptical polarized OAM modes. The experimental results of the elliptical polarized OAM modes obtained from our fiber system are in agreement with the theory results. As will be shown, situations 1, 3, and 5 describe a single arbitrary polarized OAM mode and the corresponding CV modes. Many previous works [32, 37–40, 42–44] can be included in these situations, which are some special states in the given general formulas. Situations 2, 4, and 6 describe two arbitrary orthogonal polarized OAM modes with opposite TCs [33–35, 45]. In these situations, OAM modes with opposite TCs can be separated along with the separation of their polarization, by the devices of a quarter-wave plate (QWP) and a polarizer with particular angle. It leads to the benefit that the TCs are tunable between +l and -l.

2 Theory

Before discussing the transformation relation of CV modes and OAM modes, it is helpful to know their propagating properties. Three features are given for distinguishing CV modes and OAM modes: (1) amplitude, (2) polarization state, and (3) phase. First, the radial distributions of the CV mode and OAM mode in fiber are the same, which affects the amplitude of points with different radius. The amplitudes are the same at the points with the same radius, whether in CV modes or OAM modes. Second, the polarization states of points in CV modes are always linear polarization states, while the polarized direction varies from the azimulthal angle. The polarization states of points in OAM modes are the same. Third, the phases of points in CV modes are the same or opposite (the phase when the electric vector reaches maximum is defined as the same), while that in OAM modes varies from azimulthal angle continuously. In summary, the amplitudes of CV modes and OAM modes are affected only by the radial field distribution. The polarization states vary from azimulthal angle in CV modes (and always linear polarization) and invariant in OAM modes. The phases vary from azimulthal angle in OAM modes and invariant in CV modes. Figure 1 gives the change in electric vector fields along with the propagation of two common CV modes, TE_{01} , and TM_{01} , and OAM modes, $\hat{\sigma}^-OAM_{11}$, and $\hat{x}OAM_{11}$. When propagating half a period, the trends of electric vector changes among these modes are different. For TE_{01} and TM_{01} , the polarization states at each point are linear polarization, but the polarized directions vary from the azimulthal angle. Except for the amplitude scaling factor of the points with different radius, the phases are the same, which are represented as the electric vectors changing with the same trend. For $\hat{\sigma}^-\text{OAM}_{+1}$ and $\hat{x}\text{OAM}_{+1}$, the amplitude and direction of the electric vector at each point can arrive those of another point with the same radius, but at a different time or propagation distance. In other words, for different points on the beam cross-section with the same radius, the polarization states are the same but are different in phase. Take $\hat{\sigma}^- \mathrm{OAM}_{_{\perp 1}}$ for example, shown in the third row in Figure 1; electric vectors at each point with the same radius on the beam cross-section are

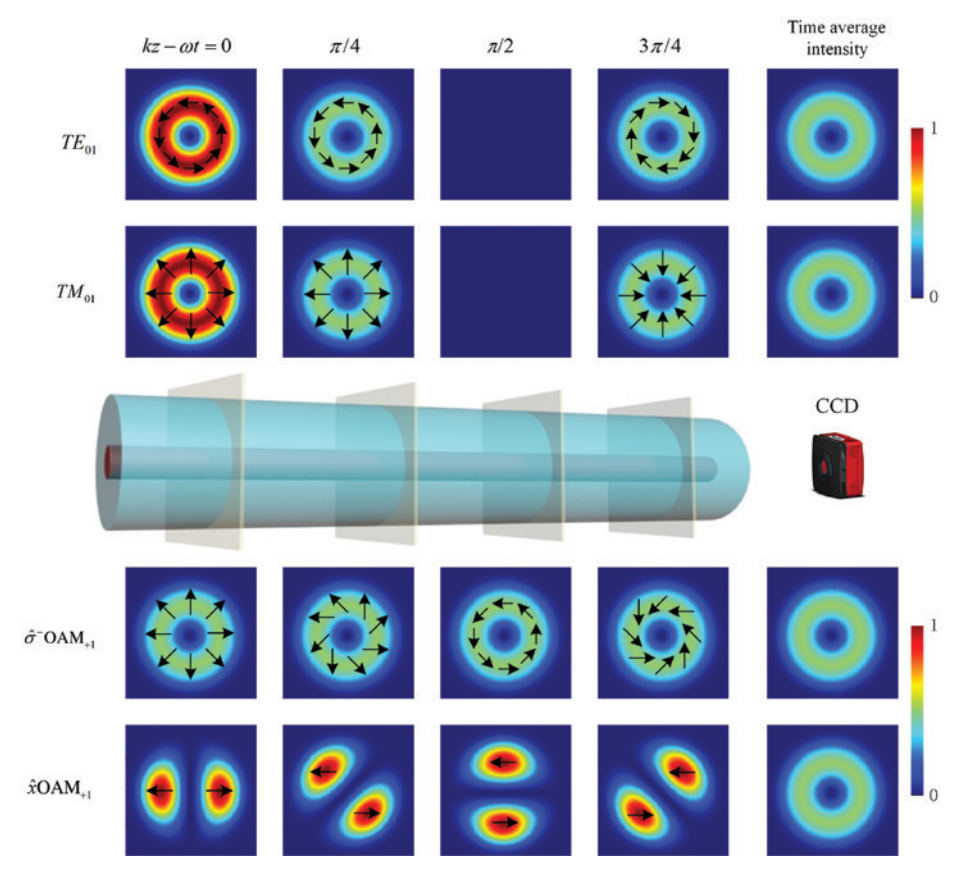


Figure 1: The electric vector field of TE_{01} , TM_{01} , $\hat{x}OAM_{+1}$, and $\hat{\sigma}^-OAM_{+1}$ along the step index fiber. $\pi/4$ phase difference is between the adjacent column. The last column figures are time-average intensity patterns in the integer period, which correspond to the patterns detected by CCD camera.

the right-hand circular polarized $(\hat{\sigma}^-)$. The phase factor of OAM_{+l} should be $e^{i(kz-\omega t+l\xi)}$. For lth-order OAM modes, the number of equal phase points on the beam cross section will be l. As shown in the third row in Figure 1, at the beginning, the x-polarization point locates at $\xi = 0(kz - \omega t + \xi = 0)$. Then, when the field propagates to $kz - \omega t = \frac{\pi}{4}$, the only x-polarization point (with the same phase) locates at $\xi = -\frac{\pi}{4}(kz - \omega t + \xi = 0)$. This means $\xi = -(kz - \omega t)$, where the equal phase point appears along with the clockwise direction when propagating, which indicates the factor $e^{i\xi}$. Thus, the third row in Figure 1 indicates $\hat{\sigma}^-$ OAM₊₁ mode. As for \hat{x} OAM₊₁, the symbol \hat{x} just indicates the linear polarization, which can be substituted by other linear polarization symbols when the observation coordinates rotate.

The figures of the last column in Figure 1 show the integer-period $(kz-\omega t=2k\pi)$ time average intensity patterns of the four modes. Because the response frequencies of the detected devices are much slower than the frequency of light, the patterns we can detect are the time average intensity patterns of a huge number of periods, which are close to the integer-period time average intensity patterns. We may notice that there is no difference among the time average intensity patterns of these four modes. To ensure phase information further, a fundamental mode is usually used to interfere with a higher-order mode from fiber. Through the interference patterns, we can get the phase information to confirm the specific electric vector field of the same doughnut intensity patterns.

A typical combination of CV modes to generate OAM mode, $\hat{\sigma}^- \text{OAM}_{+1} = TM_{01} - iTE_{01}$, is shown in Figure 1. The term " $-iTE_{01}$ " denotes the figures of the first row with $-\frac{\pi}{2}$ time delay. The physical meaning of $\hat{\sigma}^- \text{OAM}_{+1} = TM_{01} - iTE_{01}$ is the interference between TM_{01} and TE_{01} patterns with a $-\frac{\pi}{2}$ time delay of TE_{01} . In Figure 1, when TM_{01} propagates to $kz - \omega t = \frac{\pi}{2}$, TE_{01} reaches $kz - \omega t = 0$. Adding these two electric vectors, we get the $\hat{\sigma}^- \text{OAM}_{+1}$ at $kz - \omega t = \frac{\pi}{2}$. Besides $\hat{\sigma}^- \text{OAM}_{+1} = TM_{01} - iTE_{01}$, there are a series of transformation relations between CV modes and OAM modes. We are going to derive the whole relation for them.

For ideal fibers, when solving the Helmholtz equation in a cylindrical coordinate system, one can derive the electric field distribution in fibers. We use Jones calculus to express the polarization. When l > 0, the CV mode bases are

$$\begin{pmatrix} E_{x}(r,\xi,z) \\ E_{y}(r,\xi,z) \end{pmatrix} = \begin{cases}
F_{l,m}(r) \begin{pmatrix} \cos(l\xi) \\ \sin(l\xi) \end{pmatrix} e^{i\beta_{1}z}; & EH_{l-1,m}^{\text{even}} / TM_{0,m} \\
F_{l,m}(r) \begin{pmatrix} -\sin(l\xi) \\ \cos(l\xi) \end{pmatrix} e^{i\beta_{2}z}; & EH_{l-1,m}^{\text{odd}} / TE_{0,m} \\
F_{l,m}(r) \begin{pmatrix} \cos(l\xi) \\ -\sin(l\xi) \end{pmatrix} e^{i\beta_{3}z}; & HE_{l+1,m}^{\text{even}} \\
F_{l,m}(r) \begin{pmatrix} \sin(l\xi) \\ \cos(l\xi) \end{pmatrix} e^{i\beta_{4}z}; & HE_{l+1,m}^{\text{odd}}
\end{cases}$$
(1)

where $F_{lm}(r)$ is the radial field distribution, l is the azimuthal order of CV modes, m is the radial order, and β_{1-4} are the propagation constants. For l=1, $EH_{l-1,m}^{even}$ should be substituted by $TM_{0,m}$ and $EH_{l-1,m}^{\mathrm{odd}}$ should be substituted by $TE_{0,m}$. For conciseness, we use the symbol $EH_{l-1,m}^{\mathrm{even}}$ and $EH_{l-1,m}^{\text{odd}}$ to represent $TM_{0,m}$ and $TE_{0,m}$ when l=1 in the end of this section. Equation (1) indicates that for describing the electric field with a particular azimuthal order l (l>0) in fiber, at least four base vectors are needed. In other words, for a particular azimuthal order *l*, the four CV modes can be abstracted as four base vectors in a four-dimensional complex Hilbert space. OAM modes are the other four base vectors in space. Thus, OAM modes generated by CV modes are equivalent to base vector transformation in four-dimensional complex Hilbert space. For l=0, two base vectors are enough. But the 0th modes (fundamental modes) will not convert into OAM modes (or just convert into 0th order OAM modes); thus, we are not going to discuss these. In the rest of this paper, l > 0 is the default.

Because of the weak guidance of fiber, the propagation constant β of these four CV modes are almost the same. Neglecting the common complex constant $F_{l,m}(r)e^{i\beta z}$, it is convenient to convert Eq. (1) as

$$\begin{cases} EH_{l-1,m}^{\text{even}} = \frac{1}{2} \left(e^{-il\xi} \begin{pmatrix} 1 \\ i \end{pmatrix} - e^{il\xi} \begin{pmatrix} 1 \\ -i \end{pmatrix} \right); \\ EH_{l-1,m}^{\text{odd}} = -\frac{i}{2} \left(e^{-il\xi} \begin{pmatrix} 1 \\ i \end{pmatrix} - e^{il\xi} \begin{pmatrix} 1 \\ -i \end{pmatrix} \right); \\ HE_{l+1,m}^{\text{even}} = \frac{1}{2} \left(e^{-il\xi} \begin{pmatrix} 1 \\ -i \end{pmatrix} + e^{il\xi} \begin{pmatrix} 1 \\ i \end{pmatrix} \right); \\ \text{and} \\ HE_{l+1,m}^{\text{odd}} = \frac{i}{2} \left(e^{-il\xi} \begin{pmatrix} 1 \\ -i \end{pmatrix} - e^{il\xi} \begin{pmatrix} 1 \\ i \end{pmatrix} \right). \end{cases}$$
(2)

If given physical meanings, Eq. (2) can be also expressed as

$$\begin{cases} EH_{l-1,m}^{\text{even}} = \frac{1}{2} (\hat{\sigma}^{+} \text{OAM}_{-l} + \hat{\sigma}^{-} \text{OAM}_{+l}); \\ EH_{l-1,m}^{\text{odd}} = -\frac{i}{2} (\hat{\sigma}^{+} \text{OAM}_{-l} - \hat{\sigma}^{-} \text{OAM}_{+l}); \\ HE_{l+1,m}^{\text{even}} = \frac{1}{2} (\hat{\sigma}^{-} \text{OAM}_{-l} + \hat{\sigma}^{+} \text{OAM}_{+l}); \\ \text{and} \\ HE_{l+1,m}^{\text{odd}} = \frac{i}{2} (\hat{\sigma}^{-} \text{OAM}_{-l} - \hat{\sigma}^{+} \text{OAM}_{+l}), \end{cases}$$
(3)

where $\hat{\sigma}^{\pm}$ represent Jones vectors $\begin{pmatrix} 1 \\ \pm i \end{pmatrix}$ represents the field distribution of $e^{\pm il\xi}$. In ideal fibers with axisymmetric refractive index distribution, for the lthorder CV modes, the spatial electric field distribution can be expressed as $E = AEH_{l-1,m}^{\text{even}} + BEH_{l-1,m}^{\text{odd}} + CHE_{l+1,m}^{\text{even}} + DHE_{l+1,m}^{\text{odd}}$, where $(A, B, C, D)^T$ are arbitrary complex constants. The amplitudes and the phases of the complex values (A, B, $(C, D)^T$ represent the amplitudes and the relative phases of $EH_{l-1,m}^{\text{even}}$, $EH_{l-1,m}^{\text{odd}}$, $HE_{l+1,m}^{\text{even}}$, $HE_{l+1,m}^{\text{odd}}$, respectively. Equation (2) can be changed to

$$E(\xi) = \frac{1}{2} \left(e^{-il\xi} \begin{pmatrix} A + C + i(D - B) \\ D + B + i(A - C) \end{pmatrix} + e^{il\xi} \begin{pmatrix} A + C - i(D - B) \\ D + B - i(A - C) \end{pmatrix} \right)$$

$$= \frac{1}{2} \left(e^{-il\xi} \begin{pmatrix} x_{-l} \\ y_{-l} \end{pmatrix} + e^{il\xi} \begin{pmatrix} x_{+l} \\ y_{+l} \end{pmatrix} \right)$$

$$= \frac{1}{2} \left(OAM_{-l} \begin{pmatrix} x_{-l} \\ y_{-l} \end{pmatrix} + OAM_{-l} \begin{pmatrix} x_{+l} \\ y_{+l} \end{pmatrix} \right), \tag{4}$$

where $\begin{pmatrix} x_{-l} \\ y_{-l} \end{pmatrix}$ and $\begin{pmatrix} x_{+l} \\ y_{+l} \end{pmatrix}$ are Jones vectors to describe the polarization of OAM_, and OAM_, respectively. Combining the first and the second rows of Equation (4), we get the following transformation matrix:

$$\frac{1}{2} \begin{pmatrix} 1 & -i & 1 & i \\ i & 1 & -i & 1 \\ 1 & i & 1 & -i \\ -i & 1 & i & 1 \end{pmatrix} \begin{pmatrix} A \\ B \\ C \\ D \end{pmatrix} = \begin{pmatrix} x_{-l} \\ y_{-l} \\ x_{+l} \\ y_{+l} \end{pmatrix},$$
(5)

where $(A, B, C, D)^T$ and $(x_{-l}, y_{-l}, x_{+l}, y_{+l})^T$ are arbitrary complex vectors, which indicate the electric field expressed in CV mode bases and OAM mode bases. Because the coefficient matrix is nonsingular matrix, there is one and only one vector $(A, B, C, D)^T$ corresponding with any value of $(x_1, y_1, x_2, y_1)^T$, and vice versa. Figure 2 shows the intuitive sketch figure of the connection between CV mode bases and OAM mode bases. Whatever $(x_1, y_1, x_1, y_1)^T$ we want, we can get a specific combination of $(A, B, C, D)^T$



Figure 2: Sketch figure of the transformation matrix connecting *l*th CV mode bases and OAM mode bases.

by solving Equation (5). Similarly, for a specific combination of $(A, B, C, D)^T$, a group of $(x_{-1}, y_{-1}, x_{+1}, y_{+1})^T$ is defined, too. In other words, according to any desired field distribution $OAM_{-l} \begin{pmatrix} x_{-l} \\ y_{-l} \end{pmatrix} + OAM_{+l} \begin{pmatrix} x_{+l} \\ y_{+l} \end{pmatrix}$, we can calculate using Eq. (5). And for arbitrary combination of lth-order CV modes, solving Eq. (5), we can calculate the final field distribution in the bases of OAM, too.

3 Results and discussions

A fiber OAM generation system is summarized in Figure 3. The system is separated as three parts: mode couple module, field control module and polarization separation module. The mode couple module is used to couple fundamental modes to specific *l*th azimuthal order CV modes. It is generally composed of fiber grating [32, 33, 35, 38, 40, 41, 44, 46, 47] or fiber coupler [34, 45, 48, 49]. Especially by fiber grating, the couple efficiency of a single specific lth-order CV mode can reach 99%. As mentioned above, lth-order CV modes consist of four degenerated modes. Although the mode couple module has coupled fundamental mode into lth-order CV modes, the initial states of four degenerated lth-order CV modes are generally with random amplitudes and phases. The electric field generally does not satisfy the condition to the states, which can be used to generate pure OAM modes.

The field control module is used to redistribute the generated lth-order CV modes. It changes the relative amplitudes and phases among the four degenerated CV modes. In some special relations among the four degenerated vector modes, pure OAM modes can be generated, such as $\hat{\sigma}^{+}OAM_{+l} = HE_{l+1,m}^{even} + iHE_{l+1,m}^{odd}$. In fiber systems, polarization controllers (PCs) are usually used to redistribute electric field.

Polarization separation module is used to separate two orthogonal polarized OAM modes after polarization control module. It is composed of a QWP and a polarizer

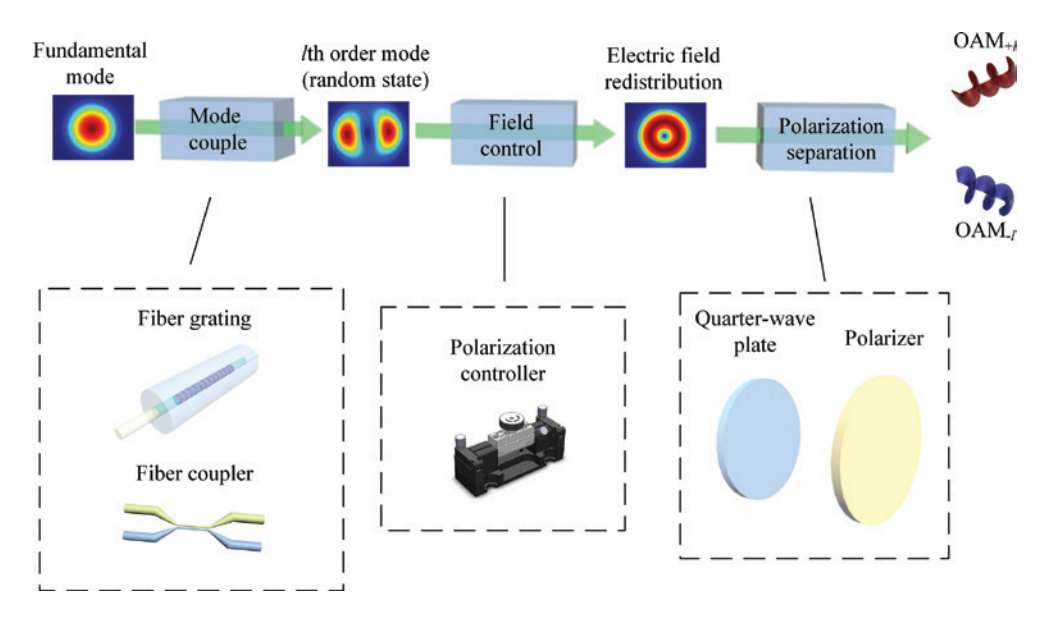


Figure 3: Sketch figure of the fiber OAM mode generation system.

with particular angle. The angle depends on the mode distribution before the polarization separation module. If the field control module generates the electric field of two orthogonal polarized OAM modes, which carry different TCs, such as $\hat{\sigma}^+ \text{OAM}_{-l} + \hat{\sigma}^- \text{OAM}_{+l}$, the two polarized orthogonal OAM modes can be separated through polarization separation module. Polarization separation module is not necessary if the electric field after polarization control module carrying pure TC.

Figure 4 shows our experiment setup. It is a fiber Mach-Zehnder interference system. An optical coupler with a splitting ratio of 5:5 is used to split the power

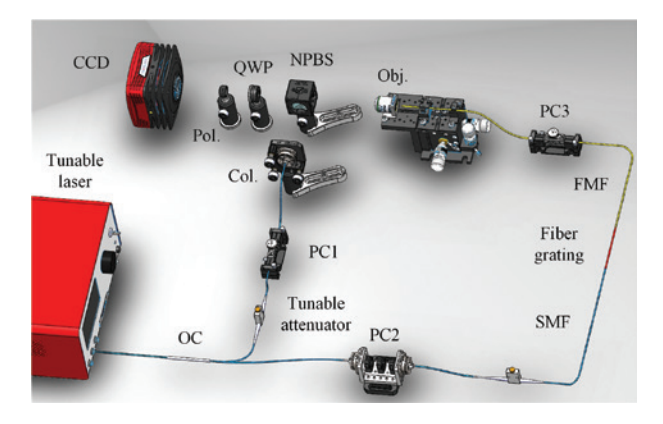


Figure 4: Experimental setup for the generation and detection of high-order modes.

OC, optical coupler; PC, polarization controller; SMF, single mode step index fiber; FMF, few modes step index fiber; Obj, objective lens; Col., collimator; NPBS, non-polarization beam splitter; QWP, quarter-wave plate; Pol, polarizer; CCD, charge coupled device.

of tunable laser (KEYSIGHT, 8164B, N7786B) into two branches. Tunable attenuators are used to adjust the power in each branch. The right branch is used to generate higher-order modes. A long period of fiber grating is used to couple fundamental modes into a particular higherorder mode. PCs are used to adjust the relative amplitudes and phases among the modes in fiber. A 40× objective lens (Obj.) is used to focus the generated higher-order mode on the charge coupled device (CCD) camera. The left branch provides fundamental modes. The fundamental mode is used to interfere with the generated higher-order mode because we need to confirm the phase information of light in the right branch through the interference patterns. Beams from two branches interfere with each other after passing through the non-polarization beam splitter. QWP and polarizer (Pol.) are used to get the information of the mode field from the right branch in different polarization directions. Finally, a CCD camera (400-1800 nm, FIND-R-SCOPE-VIS,85700) is used to record the beam patterns (with or without interference), from which we can determine the electric field from the right branch.

Next, we are going to introduce some electric field distributions in the OAM mode bases and give the general formulas to describe these situations.

As shown in Eq. (4), the electric field in fiber can be regarded as superposition of two OAM modes with opposite TCs and arbitrary polarization. Thus, we discuss all the *l*th-order electric fields as long as we discuss all polarizations of these two OAM modes. We set $(x_{-l}, y_{-l}, x_{+l}, y_{+l})^T$ as the arbitrary complex vector in four-dimensional complex space, which can be also expressed as

 $(|E_1|e^{i\delta_1}, |E_2|e^{i\delta_2}, |E_3|e^{i\delta_3}, |E_4|e^{i\delta_4})^T$. $|E_{1-\delta}|$ and $\delta_{1-\delta}$ are arbitrary real values, indicating the amplitudes and phases of x_{\perp} , y_{\perp} , x_{\perp} , y_{\perp} . As the vector in OAM mode bases been confirmed, the corresponding CV mode bases can be calculated by Eq. (5). Some situations under this general vector are given below.

3.1 A single circular polarized OAM mode

a circular polarized beam, $|E_{\bullet}| = |E_{\circ}|$ and $\delta_2 = \delta_1 + \frac{k\pi}{2}$ (k = ±1) should be satisfied (the same for $|E_{\alpha}|, |E_{\alpha}|, \delta_{\alpha}, \delta_{\alpha}$). Thus, the general vector in OAM bases to describe all states in this situation is

$$(x_{-l}, y_{-l}, x_{+l}, y_{+l})^{T} = R\left(|E_{1}|e^{i\delta_{1}}, |E_{1}|e^{i\left(\delta_{1} + \frac{k\pi}{2}\right)}, 0, 0\right)^{T}$$
or $R\left(0, 0, |E_{3}|e^{i\delta_{3}}, |E_{3}|e^{i\left(\delta_{3} + \frac{k\pi}{2}\right)}\right)^{T}$, (6)

where *R* is the rotation matrix
$$\begin{pmatrix} \cos\theta & \sin\theta & 0 & 0 \\ -\sin\theta & \cos\theta & 0 & 0 \\ 0 & 0 & \cos\theta & \sin\theta \\ 0 & 0 & -\sin\theta & \cos\theta \end{pmatrix}$$

where θ is the arbitrary constant. θ depends on the angle of the selected coordinates. The value of θ does not change the physical meaning but changes the expression. If given physical meanings, Eq. (6) can be expressed as an equivalent form as Eq. (4),

$$E(\xi) = \left| E_1 \right| e^{i\delta_1} \begin{pmatrix} 1 \\ \pm i \end{pmatrix} \text{OAM}_{-l} \text{ or } \left| E_3 \right| e^{i\delta_3} \begin{pmatrix} 1 \\ \pm i \end{pmatrix} \text{OAM}_{+l}. \tag{7}$$

Eq. (7) indicates a single circular polarized OAM mode with arbitrary amplitude and phase. That is why Eq. (6) includes all the single circular polarized OAM mode situations. In other words, any electric field that can be

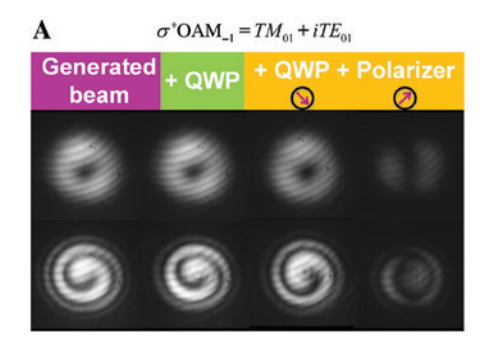
expressed by Eq. (6) is a single circular polarized OAM mode. For example, $\hat{\sigma}^+OAM_{_{-1}}$ can be expressed as $(x_{_{-1}}, y_{_{-1}}, y_{_{-1}}, y_{_{-1}}, y_{_{-1}}, y_{_{-1}})$ $(x_{+1}, y_{+1})^T = (1, i, 0, 0)^T$, where $|E_1| = 1, \delta_1 = 0, \theta = 0$, and k = 1. We get

$$E(\xi) = e^{-il\xi} \begin{pmatrix} 1 \\ i \end{pmatrix} = \hat{\sigma}^{+} \text{OAM}_{-l}.$$
 (8)

It is a left-hand circular polarized OAM mode with TC -l. Substituting this vector into Eq. (5), we get $(A, B, C, D)^T$ = $(1, i, 0, 0)^T$. It This indicates that the electric field expressed in CV mode bases is $EH^{\mathrm{even}}_{l-1,m}+iEH^{\mathrm{odd}}_{l-1,m}(TM_{_{0,m}}+iTE_{_{0,m}} \text{ for } l=1).$

Similarly, $(x_{-i}, y_{-i}, x_{+i}, y_{+i})^T = (1, -i, 0, 0)^T$, a pure righthand circular polarized OAM mode with TC -l, corresponds with $(A, B, C, D)^T = (0, 0, 1, -i)^T$. It is $HE_{l+1,m}^{\text{even}} - iHE_{l+1,m}^{\text{odd}}$ in the bases of CV modes. If we set $(x_{-1}, y_{-1}, x_{+1}, y_{+1})^T = (0, 0, 0)$ 1, $\pm i$)^T, a circular polarized OAM mode with TC +l, we will get similar results in the same analysis method.

In our previous work [32], we have researched these states. We used long period fiber grating to couple fundamental modes into the first- and second-order CV modes. The experiment device is similar to that shown in Figure 4. The experiment results are shown in Figure 5. We define ψ as the counterclockwise angle from the slow axis of QWP to the axis of polarizer. And we fix the fast axis of QWP on the y-axis. The two rows in Figure 5 show the patterns without interference (intensity patterns) and with interference (interference patterns). The first column shows the patterns without passing-through QWP and polarizer. The second column shows the patterns with a single QWP. The last two columns show the patterns with QWP and polarizer where $\psi = -45^{\circ}$ and 45° , respectively. Because QWP is able to change arbitrary polarization into linear polarization, we can judge the origin polarization from the angle ψ . When $\psi = 45^{\circ}$, the intensity pattern vanishes, which indicates the polarization to be left-handed circular $\hat{\sigma}^+$ The interference pattern is clockwise vortex, indicating the phase factor $e^{-il\xi}$. Thus, the origin mode should be $\hat{\sigma}^+$ OAM ,.



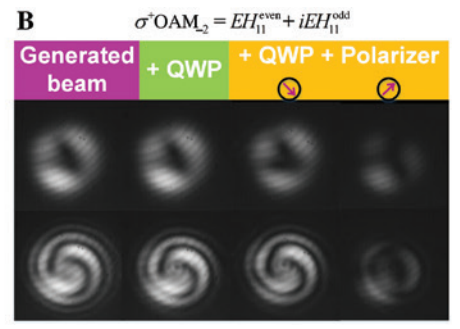


Figure 5: Intensity and interference patterns of circular polarized OAM modes. (A) $\hat{\sigma}^+$ OAM₋₁ and (B) $\hat{\sigma}^+$ OAM₋₂. The title is the corresponding expression in CV mode bases and OAM mode bases.

As can be seen, $\hat{\sigma}^+ \text{OAM}_{-l} = \text{EH}^{\text{even}}_{l-1,m} + iEH^{\text{odd}}_{l-1,m}$ corresponding to a special value of $|E_1|=1$, $\delta_1=0$, and k=+1 in the general vector Eq. (6). Indeed, $|E_1|$, δ_1 can be arbitrary values, and k can be ± 1 . Equation (6) may be more universal, which concludes all the circular polarized OAM modes and their corresponding CV modes. A few articles belong to this situation [32, 38, 39, 41, 43].

3.2 Two orthogonal circular polarized OAM modes with opposite TCs

Besides the restriction of circular polarization as shown in Situation 1, an extra restriction should be added that the two OAM modes with opposite TCs are orthogonal in polarization. That is, $x_{-l}^* x_{+l} + y_{-l}^* y_{+l} = 0$ should be satisfied. Thus, the general vector in OAM bases to describe all states in this situation is

$$(x_{-l}, y_{-l}, x_{+l}, y_{+l})^{T} = R \left(|E_{1}| e^{i\delta_{1}}, |E_{1}| e^{i\left(\delta_{1} + \frac{k\pi}{2}\right)}, -|E_{3}| e^{i\delta_{3}}, |E_{3}| e^{i\left(\delta_{3} - \frac{k\pi}{2}\right)} \right)^{T}.$$

$$(9)$$

Consider the vector in the OAM mode bases $(x_{-l}, y_{-l}, x_{+l}, y_{+l})^T = (-0.5i, 0.5, 0.5i, 0.5)^T$, where $|E_1| = |E_3| = 0.5$, $\delta_1 = -\frac{\pi}{2}$, $\delta_3 = \frac{\pi}{2}$, $\theta = 0$, and k = 1. $E(\xi)$ is

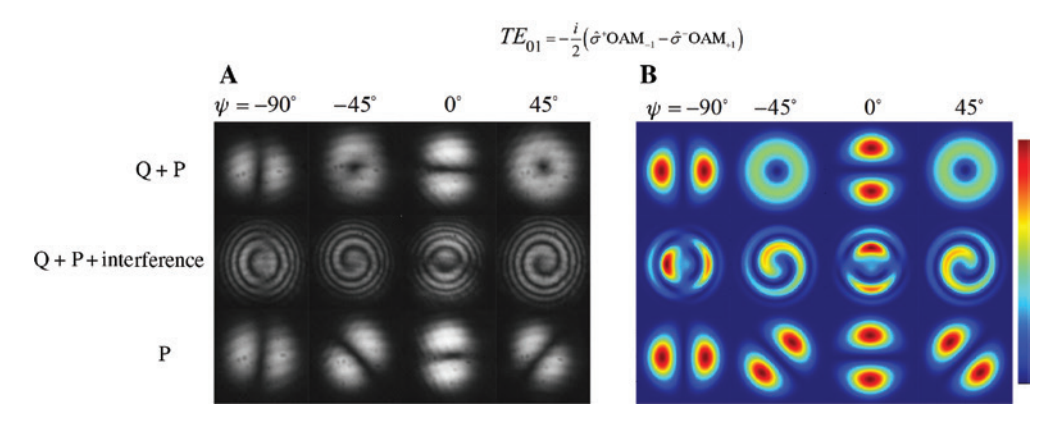
$$E(\xi) = \frac{i}{2} \left(-e^{-il\xi} \begin{pmatrix} 1 \\ i \end{pmatrix} + e^{il\xi} \begin{pmatrix} 1 \\ -i \end{pmatrix} \right)$$
$$= \frac{i}{2} \left(-\hat{\sigma}^{+} OAM_{-l} + \hat{\sigma}^{-} OAM_{+l} \right). \tag{10}$$

Substituting this vector into Eq. (5), we get $(A, B, C, D)^T = (0, 1, 0, 0)^T$. This situation corresponds to a pure $TE_{0,m}/EH_{l-1,m}$ mode. As shown in Eq. (3), a pure CV mode can be regarded as a superposition of two OAM modes with opposite TCs. And their polarized states are orthogonal. Arbitrary orthogonal polarized beams can be transformed into two linear orthonormal polarized beams by a QWP. Thus, we can use a QWP and a polarizer to separate these two beams. Figure 6 shows the intensity and interference patterns of this situation. We still set the fast axis of the QWP as the *y*-axis. When passing through the

QWP, $\hat{\sigma}^+\text{OAM}_{-l}$ is transformed into $\begin{pmatrix} 1 \\ -1 \end{pmatrix} \text{OAM}_{-l}$, a -45° LP OAM beam, while $\hat{\sigma}^-\text{OAM}_{+l}$ is transformed into $\begin{pmatrix} 1 \\ 1 \end{pmatrix} \text{OAM}_{+l}$, a 45° LP OAM beam. The intensities of OAM_{-l} and OAM_{+l} are almost the same. If we set a polarizer or birefringent crystal behind the QWP with $\psi = \pm 45^\circ$, we can separate these two orthogonal LP states. Their carried opposite TCs are separated simultaneously. At other ψ angles, the states cannot be expressed by a single OAM mode. The interference pattern does not appear at the pure vortex property at these ψ angles. They are hybrid OAM mode states. As shown in Figure 6, when $\psi = 0^\circ$ or 90° , the patterns do not present the properties of the OAM mode. It is the pattern

The phase difference between OAM_{-l} and OAM_{+l} is hinted at the intensity patterns at $\psi=0^{\circ}$ or 90° , which can be regarded as the interferece of OAM_{-l} and OAM_{+l} . Take $\psi=0$ for example; after passing through the QWP, the mode field should be

$$E_{Q} = e^{-il\xi} \begin{pmatrix} 1 \\ -1 \end{pmatrix} + e^{i(l\xi + \alpha)} \begin{pmatrix} 1 \\ 1 \end{pmatrix}, \tag{11}$$



of pure LP modes.

Figure 6: Intensity and interference patterns of the generated hybrid state combined by two orthogonal circular polarized OAM modes, which carry opposite TCs.

(A) Experimental results. (B) Corresponding simulations. The title is the corresponding expression in CV mode bases and OAM mode bases. ψ is the counterclockwise angle from the slow axis of QWP to the polarizer. The fast axis of the QWP locates on the *y*-axis.

where α is the phase difference between OAM, and OAM, When inserting a polarizer, the mode field should be

$$E_{QP} = \begin{pmatrix} \cos \psi & -\sin \psi \\ \sin \psi & \cos \psi \end{pmatrix} \begin{pmatrix} 1 & 0 \\ 0 & 0 \end{pmatrix} \begin{pmatrix} \cos \psi & \sin \psi \\ -\sin \psi & \cos \psi \end{pmatrix} E_{Q}$$

$$= 2e^{\frac{i\alpha}{2}} \begin{pmatrix} \cos \left(l\xi + \frac{\alpha}{2} \right) \\ 0 \end{pmatrix}$$
(12)

The intensity of the final field after QWP and polarizer should be $I \propto \left| E_{QP} \right|^2 = 4\cos^2\left(l\xi + \frac{\alpha}{2}\right)$. When I reaches the maximum, $\cos^2\left(l\xi + \frac{\alpha}{2}\right)$ should be 1, where $\xi = \frac{-\frac{\alpha}{2} + k\pi}{l}$ $\xi = -\frac{\alpha}{2} + k\pi$ for l=1. Going back to Figure 6, when

 $\psi = 0$, the maximum of intensity pattern locates at $\xi = \frac{\pi}{2}$.

Thus, the phase difference between OAM_{-l} and OAM_{+l} , α is calculated to be $\pi + 2k\pi$. The same α value can be calculated at $\psi = 90^{\circ}$.

Thus,
$$E_Q = e^{-il\xi} \begin{pmatrix} 1 \\ -1 \end{pmatrix} - e^{il\xi} \begin{pmatrix} 1 \\ 1 \end{pmatrix}$$
. The original field before

passing through the QWP is

$$E = \begin{pmatrix} 1 & 0 \\ 0 & -i \end{pmatrix} E_Q = \begin{pmatrix} -\sin l\xi \\ \cos l\xi \end{pmatrix} = TE_{01} / EH_{l-1,m}^{\text{odd}}, \tag{13}$$

where we neglect the common amplitude and phase factor before Jones matrix because they do not affect the final result. The last row in Figure 6 shows the common verification of TE_{01} mode, by inserting a polarizer only.

For another example, $(x_{-1}, y_{-1}, x_{+1}, y_{+1})^T = (0.5i, 0.5, -0.5i,$ $(0.5)^T$ also satisfies the general vector. It corresponds to $(A, A, A, A)^T$ $B, C, D)^T = (0, 0, 0, 1)^T$, which indicates a pure $HE_{l+1, m}^{\text{odd}}$. And some similar situations can be derived in the same process. Notice that the pure CV modes are some, but not all, states of situation 2. There are a series of states satisfying Eq. (9)

besides the pure CV modes. In our previous work, Han has found the relation TM_{01} , TE_{01} , $TM_{01} + TE_{01}$, and $TM_{01} - TE_{01}$ and their corresponding CV modes [35]. There are several special states under this situation. Any vector satisfying Eq. (9) belongs to this situation.

3.3 A single LP OAM mode

For an LP beam, $\delta_2 = \delta_1 + k\pi(k=0, 1)$ should be satisfied (the same for δ_a , and δ_a). The general vector in OAM bases to describe all states in this situation is

$$(x_{-l}, y_{-l}, x_{+l}, y_{+l})^{T} = R(|E_{1}|e^{i\delta_{1}}, |E_{2}|e^{i(\delta_{1}+k\pi)}, 0, 0)^{T}$$
or $R(0, 0, |E_{3}|e^{i\delta_{3}}, |E_{4}|e^{i(\delta_{3}+k\pi)})^{T}$. (14)

Consider the vector in the OAM mode bases (x_{-l}, y_{-l}, x_{+l} , $(y_1)^T = (1, 0, 0, 0)^T$, where $|E_1| = 1$, $|E_2| = 0$, $\delta_1 = 0$, $\theta = 0$, and k=0. $E(\xi)$ is

$$E(\xi) = e^{-il\xi} \begin{pmatrix} 1 \\ 0 \end{pmatrix} = \hat{x} OAM_{-l}.$$
 (15)

Substituting this vector into Eq. (5), we get $(A, B, C, D)^T = (0.5, 0.5i, 0.5, -0.5i)^T$. The state is $0.5EH_{l-1,m}^{\mathrm{even}} + 0.5iEH_{l-1,m}^{\mathrm{odd}} + 0.5HE_{l+1,m}^{\mathrm{even}} - 0.5iHE_{l+1,m}^{\mathrm{odd}} (0.5TM_{01} + 0.5iTE_{01} + 0.5HE_{21}^{\mathrm{even}} - 0.5iHE_{21}^{\mathrm{odd}}$ for l=1). The electric field is also equivalent to $\hat{x}LP_{l,m}^{\mathrm{even}} - i\hat{x}LP_{l,m}^{\mathrm{odd}}$. The symbol LP represents LP modes, which are another group of bases to describe the electric field in fibers. In this paper, we are not going to discuss LP modes in detail. It is a special situation in which the QWP can be neglected because the states are intrinsic linear polarization. That is, we can observe the intensity vanishing without the assistance of QWP. When the QWP is removed, ψ loses the original definition (the counterclockwise angle from the slow axis of QWP to the axis of polarizer). We can define $\psi = 0$ on arbitrary axis. Figure 7 gives the first-order (l=1) intensity

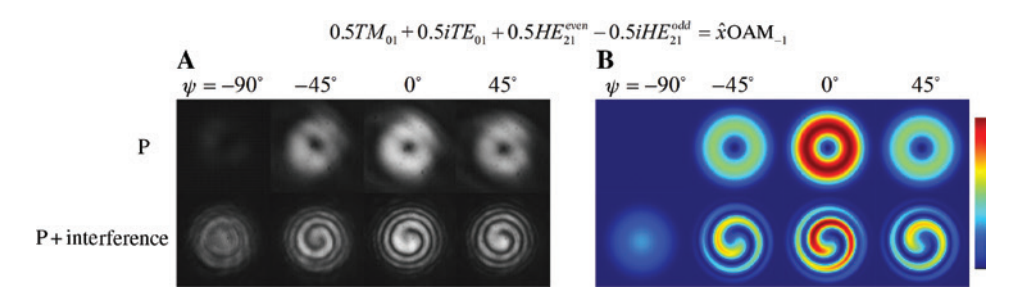


Figure 7: Intensity and interference patterns of a single linear OAM mode (after passing through a QWP and polarizer). (A) Experimental results. (B) Corresponding simulations. The title is the corresponding expression in CV mode bases and OAM mode bases.

and the interference patterns of this state in experiment and simulation, which corresponds well with we have discussed above. Here, \hat{x} just represents the linear polarization, which can be substituted by other linear polarization symbols when the observation coordinates rotate (with different rotation factor R).

Li et al. [40] using a mechanical long period fiber grating, realized the first-order LP OAM modes, $\hat{x}(\hat{y})OAM_{\pm 1} = \hat{x}(\hat{y})LP_{11}^{\text{even}} \pm i\hat{x}(\hat{y})LP_{11}^{\text{odd}}$. Wu et al. [37] extended this relation to the second order, that is, $\hat{x}(\hat{y})OAM_{\pm 2} = \hat{x}(\hat{y})LP_{21}^{\text{even}} \pm i\hat{x}(\hat{y})LP_{21}^{\text{odd}}$. These results [36, 37, 40, 42, 44] are some special states included by Eq. (14).

3.4 Two orthogonal LP OAM modes with opposite TCs

Similar to situation 2, besides the restriction of linear polarization $\delta_2 = \delta_1 + k\pi(k=0,1)$, the restriction of orthogonal polarization $x_{-l}^* x_{+l} + y_{-l}^* y_{+l} = 0$ should be satisfied too. The general vector in OAM bases to describe all states in this situation is

$$(x_{-l}, y_{-l}, x_{+l}, y_{+l})^{T} = R(|E_{1}|e^{i\delta_{1}}, |E_{2}|e^{i(\delta_{1}+k\pi)}, -F|E_{2}|e^{i(\delta_{3}-k\pi)}, F|E_{1}|e^{i\delta_{3}})^{T},$$
(16)

where *F* is an arbitrary complex constant. Consider the vector in the OAM mode bases $(x_{-l}, y_{-l}, x_{+l}, y_{+l})^T = (0, i, 1, 0)^T$,

where
$$|E_1|=0$$
, $|E_2|=1$, $\delta_1=\frac{\pi}{2}$, $\delta_3=0$, $F=-1$, $\theta=0$, $k=0$. $E(\xi)$ is

$$E(\xi) = ie^{-il\xi} \begin{pmatrix} 0 \\ 1 \end{pmatrix} + e^{il\xi} \begin{pmatrix} 1 \\ 0 \end{pmatrix} = i\hat{y}OAM_{-l} + \hat{x}OAM_{+l}. \tag{17}$$

Substituting this vector into Eq. (5), we get $(A, B, C, D)^T = (1, 0, 0, i)^T$. The electric field is $EH^{\mathrm{even}}_{l-1,m} + iHE^{\mathrm{odd}}_{l-1,m} (TM_{0,m} + iHE^{\mathrm{odd}}_{2,m} \text{ for } l = 1)$ in CV mode bases. The constant i before $\hat{y}\mathrm{OAM}_{-l}$ just represents the

relative phase between $\hat{x}\text{OAM}_{-l}$ and $\hat{y}\text{OAM}_{+l}$, which will not affect the separation of these two OAM modes (0° and 90°) but affects the pattern at other angles. The phase difference between OAM_{+l} and OAM_{-l} is $\frac{\pi}{2}$, where the calculated method is given in Section 3.2. Figure 8 shows the corresponding state. In this situation, the QWP is not needed because the polarization is intrinsic linear. The opposite TCs can be separated by a polarizer, as mentioned in situation 2.

Jiang et al. [33, 34] and Yao et al. [45] have researched the states $\hat{x}OAM_{\mp 1} \pm i\hat{y}OAM_{\pm 1} = TE_{01} \mp iHE_{21}^{\text{even}}$ and $\hat{x}OAM_{\pm 1} \pm i\hat{y}OAM_{\mp 1} = TM_{01} \pm iHE_{21}^{\text{odd}}$ yet, which are some special states of the general vector Eq. (15). Their experiment setup is similar to Figure 4, but without the QWP. The other difference is that they use an extrusion long-period grating to couple the fundamental modes into the first order modes. It should be underlined that their theory model is a little different from ours. We set TE_{01} as $(-\sin\xi,\cos\xi)^T$ while they set TE_{01} as $-(-\sin\xi,\cos\xi)^T$. The two models are both allowed, but TE_{01} in our model should be substituted into $-TE_{01}$ in their model. $TE_{01} \mp iHE_{21}^{\text{even}}$ is the expression in our model but $-TE_{01} \mp iHE_{21}^{\text{even}}$ in their model. The other results are the same. These results [33, 34, 45] are the several special states included by Eq. (16).

3.5 A single elliptical polarized OAM mode

The general vector in OAM bases to describe all states in this situation is

$$(x_{-l}, y_{-l}, x_{+l}, y_{+l})^T = R(|E_1|e^{i\delta_1}, |E_2|e^{i\delta_2}, 0, 0)^T$$

or $R(0, 0, |E_3|e^{i\delta_3}, |E_4|e^{i\delta_4})^T$, (18)

where $\delta_1 \neq \delta_2 + k\pi$ (k = 0, 1) (linear polarization if unsatisfied, situation 1) and $\delta_1 \neq \delta_2 + \frac{k\pi}{2}$ ($k = \pm 1$) when

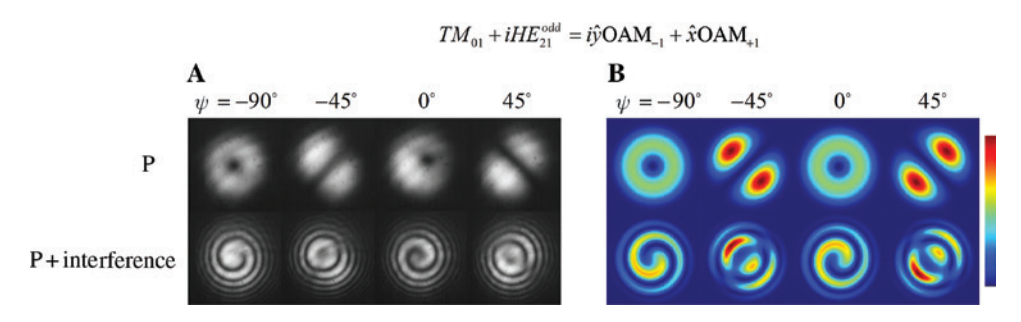


Figure 8: Intensity and interference patterns of the generated elliptical polarized OAM mode (after passing through a polarizer).

(A) Experimental results. (B) Corresponding simulations. The title is the corresponding expression in CV mode bases and OAM mode bases.

 $|E_1| = |E_2|$ (circular polarization if unsatisfied, situation 3). $|E_1|$, $|E_2|$, δ_1 , and δ_2 can be any value except these. If $|E_1|$, $|E_2|$, δ_1 , and δ_2 satisfy this restriction (the same for $|E_3|$, $|E_{\alpha}|$, δ_{α} , and δ_{α}), the electric field described by Eq. (18) is a single elliptical polarized OAM mode.

Consider the vector in the OAM mode bases $(x_1, y_1, x_2, x_3, y_4)^T = (0.24, 0.97i, 0, 0)^T,$ where $|E_1| = 0.24$, $|E_2| = 0.97$, $\delta_1 = 0$, $\delta_2 = \frac{\pi}{2}$, $\theta = 0$, $E(\xi)$ is

$$E(\xi) = e^{-il\xi} \begin{pmatrix} 0.24 \\ 0.97i \end{pmatrix}. \tag{19}$$

In this situation, solving Eq. (5), we get (A, B, C, C, C) $D)^{T} = (0.61, 0.61i, -0.37, 0.37i)^{T}$. If setting l = 1, the electric field is $0.61TM_{01} + 0.61iTE_{01} - 0.37HE_{21}^{\text{even}} + 0.37iHE_{21}^{\text{odd}}$ expressed in CV mode bases. After passing through the QWP, the electric field should be $\begin{pmatrix} 1 & 0 \\ 0 & i \end{pmatrix} \begin{pmatrix} 0.24 \\ 0.97i \end{pmatrix} e^{-il\xi} = \begin{pmatrix} 0.24 \\ -0.97 \end{pmatrix} e^{-il\xi}$, which indicates a -76° LP OAM mode with TC = -l. Thus, the polarizer should be placed at $\psi = 14^{\circ}$ to make the pattern vanish, which is different with ±45° in situation 1 (circular polarized OAM modes) and 0° or 90° in situation 3 (LP OAM modes). Figure 9 gives the experiment and simulation results of this state. The intensity pattern vanishes after passing through the QWP and polarizer with $\psi = 14^{\circ}$ and reaches a maximum when $\psi = -76^{\circ}$.

It is obvious that, unlike the discrete spin angular momentum = -1, 0, 1 mentioned in previous works, the polarized states of OAM modes should be continuous. Between linear and circular polarized OAM modes, there should be a series of continuous elliptical polarized OAM modes. The specific polarization of OAM mode can be confirmed by the ψ angle at which the pattern intensity vanishes. These states have not been reported in fiber OAM systems.

3.6 Two orthogonal elliptical polarized OAM modes with opposite TCs

Similar to situations 2 and 4, besides satisfying the restriction in situation 5 $(\delta_1 \neq \delta_2 + k\pi (k=0, 1))$ and $\delta_1 \neq \delta_2 + \frac{k\pi}{2}(k = \pm 1) \text{ when } |E_1| = |E_2|, \qquad x_{-l}^* x_{+l} + y_{-l}^* y_{+l} = 0$

should be satisfied. The general vector in OAM bases to describe all states in this situation should be

$$(x_{-l}, y_{-l}, x_{+l}, y_{+l})^{T} = R(|E_{1}|e^{i\delta_{1}}, |E_{2}|e^{i\delta_{2}}, -F|E_{1}|e^{-i\delta_{2}}, F|E_{1}|e^{-i\delta_{1}})^{T}.$$
(20)

Consider the vector in the OAM mode bases $(x_1, y_1, y_2, y_3, y_4, y_5)$ $(x_1, y_1)^T = (0.83, -0.56i, 0.56e^{1.68i}, 0.83ie^{1.68i})^T$, where $|E_1| = 0.83$, $|E_2| = 0.56$, $\delta_1 = 0$, $\delta_2 = -\frac{\pi}{2}$, $F = e^{\left[1.68 + \frac{\pi}{2}\right]}$, and $\theta = 0$. $E(\xi)$ is

$$E(\xi) = e^{-il\xi} \begin{pmatrix} 0.83 \\ -0.56i \end{pmatrix} + e^{il\xi} e^{1.68i} \begin{pmatrix} 0.56 \\ 0.83i \end{pmatrix}.$$
 (21)

It is a hybrid state of two orthogonal elliptical polarized OAM modes carrying opposite TCs. When passing through the OWP, whose fast axis locates on v-axis, the electric field becomes

$$E(\xi) = e^{-il\xi} \begin{pmatrix} 0.83 \\ 0.56 \end{pmatrix} + e^{il\xi} e^{1.68i} \begin{pmatrix} 0.56 \\ -0.83 \end{pmatrix}.$$
 (22)

The left term indicates a 34° LP OAM mode with TC = -l, while the right term indicates a -56° LP OAM mode with TC = +l. They can be separate by a polarizer or a birefringent crystal, as mentioned above. The first-order (TC = ± 1) results are shown in Figure 10. The corresponding expression in CV mode bases is $(A, B, C, D)^T = (0.14e^{-0.73i}, 0.13e^{2.41i},$ $0.66e^{0.84i}$, $0.73e^{-2.30i}$)^T. Obviously, this situation is more complicated than the linear and circular polarized OAM modes as shown in situations 2 and 4. However, elliptical

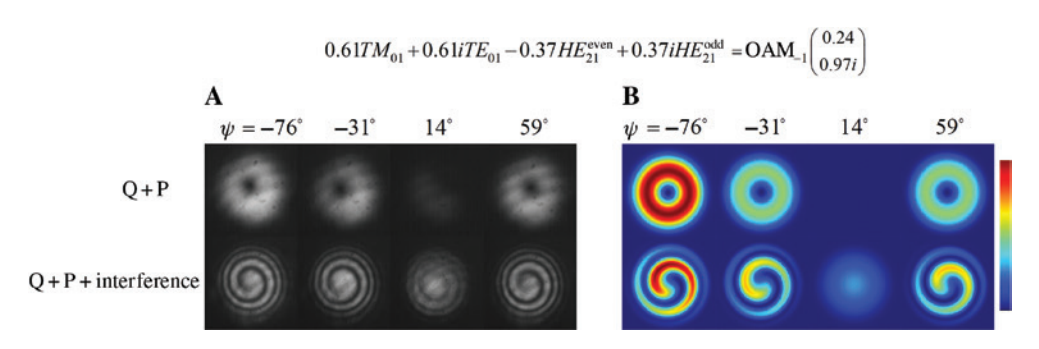


Figure 9: Intensity and interference patterns of the generated elliptical polarized OAM mode (after passing through a QWP and polarizer). (A) Experimental results. (B) Corresponding simulations. The title is the corresponding expression in CV mode bases and OAM mode bases. ψ is the counterclockwise angle from the slow axis of QWP to the polarizer. The fast axis of the QWP locates on the y-axis.

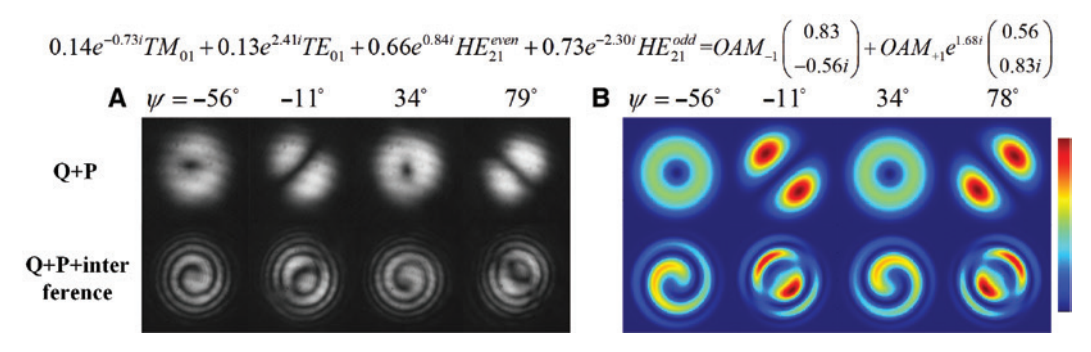


Figure 10: Intensity and interference patterns of the generated two orthogonal elliptical polarized OAM modes, which carry opposite TCs. (A) Experimental results. (B) Corresponding simulations. The title is the corresponding expression in CV mode bases and OAM mode bases. ψ is the counterclockwise angle from the slow axis of QWP to the polarizer. The fast axis of the QWP locates on the γ -axis.

polarization is the most common polarization in reality. It is meaningful to discuss elliptical polarized OAM modes.

The six situations have been discussed already and a short conclusion is given below.

Situations 1, 3, and 5 give pure circular, linear, and elliptical polarized OAM modes. These situations provide a single pure OAM mode generated by the combination of CV modes directly, which is convenient and simple. Situations 2, 4, and 6 give hybrid states in which two orthogonal circular, linear, and elliptical polarized modes carry opposite TCs. If satisfying $x_{-l}^* x_{+l} + y_{-l}^* y_{+l} = 0$, the two polarized modes in Jones vector $\begin{pmatrix} x_{-l} \\ y_{-l} \end{pmatrix}$ and $\begin{pmatrix} x_{+l} \\ y_{+l} \end{pmatrix}$ are orthogonal and can be separated by cooperation of a QWP and a polarizer with particular intersection angle. We can derive the specific polarization through the intersection angle. When

with particular intersection angle. We can derive the specific polarization through the intersection angle. When the polarizations have been separated, the TCs are separated too. These situations may lead to an extra benefit. The TCs are adjustable by the polarizer.

Each situation has their general vector to describe all their states. In these six situations, circular polarized and LP OAM modes (situations 1-4), have been reported in many papers [32-45], which are some particular states of Eqs. (6), (9), (14), and (16). In more general situations, elliptical polarized OAM modes have not been reported in fiber OAM systems. We discuss these elliptical polarized OAM modes in detail and find their corresponding CV modes. As we can see in situations 5 and 6, the corresponding CV modes of elliptical polarized OAM modes are a little complicated so that we cannot judge the physical properties directly. It is hard but meaningful to discuss these states in detail because elliptical polarization is the most universal state in reality. We give a procedure to analyze these states more intuitively. One just needs to find the situation of the OAM modes of interest, express it in the corresponding general vector in situations 1-6, and substitute it into Eq. (5). The corresponding CV modes of the OAM modes can be calculated. It should be noticed that the general

vectors $(x_{-l}, y_{-l}, x_{+l}, y_{+l})^T$ restricted by situations 1–6 do not fill each point of four-dimensional complex space. In other words, the states in situations 1–6 are not all the states that can describe the arbitrary combination of CV modes. There are still many states that may be used. Besides, situations 1–4 are enough to describe most transformation relations that have been reported. We are going to study the other situations and pick some useful states in our further work.

As has been mentioned above, the propagation constants $\beta_{\text{1--4}}$ of these four CV modes are almost the same but are not. A more accurate model should consider the difference of β at the same time. In ideal fibers, the propagation constants of even mode and odd mode with the same order are exactly equal for any CV mode. For example, $\beta_{EH_{5,3}^{\text{even}}} = \beta_{EH_{5,3}^{\text{odd}}}$. Meanwhile, β is generally different among any other modes. For example, $\beta_{EH_{5,3}^{\text{even}}} \neq \beta_{EH_{6,3}^{\text{even}}} \neq \beta_{HE_{6,3}^{\text{even}}}$. And for $TM_{0,m}$ and $TM_{0,m}$, their propagation constants are not equal. Equation (5) should be corrected as

$$\frac{1}{2} \begin{pmatrix} 1 & -i & 1 & i \\ i & 1 & -i & 1 \\ 1 & i & 1 & -i \\ -i & 1 & i & 1 \end{pmatrix} \begin{pmatrix} Ae^{i\beta_{1}z} \\ Be^{i\beta_{2}z} \\ Ce^{i\beta_{3}z} \\ De^{i\beta_{4}z} \end{pmatrix} = \begin{pmatrix} x_{-l} \\ y_{-l} \\ x_{+l} \\ y_{+l} \end{pmatrix}.$$
(23)

If OAM modes are generated by several CV modes with different propagation constants. The OAM modes can not propagate at a long distance because it will lead to a state change. Take the situation $EH^{\mathrm{even}}_{l-1,m}+iEH^{\mathrm{odd}}_{l-1,m}(TM_{0,m}+iTE_{0,m} \text{ for } l=1)$ for an example. Back to Eq. (4), the electric field of $E(\xi,z)$ should be

$$\begin{split} E(\xi,z) &= \frac{1}{2} e^{-il\xi} \binom{1}{i} (e^{i\beta_1 z} + e^{i\beta_2 z}) + \frac{i}{2} e^{il\xi} \binom{1}{-i} (-e^{i\beta_1 z} + e^{i\beta_2 z}) \\ &= e^{-il\xi} \binom{1}{i} e^{i\frac{\beta_1 + \beta_2}{2} z} \cos \left(\frac{\beta_1 - \beta_2}{2} z \right) \\ &+ i e^{il\xi} \binom{1}{-i} e^{i\frac{\beta_1 + \beta_2}{2} z} \sin \left(\frac{\beta_1 - \beta_2}{2} z \right) \end{split}$$

$$= \left(\hat{\sigma}^{+} OAM_{-l} \cos\left(\frac{\beta_{1} - \beta_{2}}{2}z\right)\right) + i\hat{\sigma}^{-} OAM_{+l} \sin\left(\frac{\beta_{1} - \beta_{2}}{2}z\right) e^{i\frac{\beta_{1} + \beta_{2}}{2}z}. \tag{24}$$

 $\cos\left(\frac{\beta_1-\beta_2}{2}z\right)$ and $\sin\left(\frac{\beta_1-\beta_2}{2}z\right)$ are the envelopes of $\hat{\sigma}^+ OAM_{\perp l}$ and $\hat{\sigma}^- OAM_{\perp l}$. At the start,

$$\begin{cases} \cos\left(\frac{\beta_1 - \beta_2}{2}z\right) = 1\\ \sin\left(\frac{\beta_1 - \beta_2}{2}z\right) = 0 \end{cases}$$
, the electric field $E(\xi, z)$ has a pure

TC -l. While transmitting to
$$z_{\text{walk-off}} = \frac{\pi}{\beta_1 - \beta_2} = \frac{\lambda}{2\Delta n_{\text{eff}}}$$
,
$$\begin{cases} \cos\left(\frac{\beta_1 - \beta_2}{2}z\right) = 0\\ \sin\left(\frac{\beta_1 - \beta_2}{2}z\right) = 1 \end{cases}$$
, $E(\xi, z)$ has a pure TC +l. It means that

if we generate the OAM mode through combining several CV modes in different values of β , the TC of the OAM mode is not invariant along with propagation distance but has a period change of $\pm l$. The walk-off length will be shorter along with the increased difference of effective refractive index Δn_{eff} Take TE_{01} and TM_{01} in most of commercial step index fibers, for example, at the wavelength $\lambda = 1.55 \mu m$, the typical value of effective refractive index $\Delta n_{\rm eff} \approx 10^{-6}$, $z_{
m walk-off}{pprox}$ 0.775 m. This means that TC changes from one state to the opposite at meter-scale. It indicates that OAM modes combined by TE_{01} and TM_{01} are unstable when propagating a long distance. Moreover, if the source produces pulse light, when propagating a distance, TE_{o1} and TM₀₁ will stagger in time domain and will not interfere anymore. Thus, it is better to use CV modes with smaller $\Delta n_{\rm eff}$ to combine the needed OAM mode.

In ideal fibers, any even and odd modes are degenerated in theory. However, in reality, fibers always suffer intrinsic defects and external perturbations, such as stress, bending, heating, twisting, and so on. These factors may affect the weak guiding property in a degree and lead to a larger $\Delta n_{\rm off}$. Chen and Wang [50] has studied these factors. For 100 mode step index multimode fibers, when suffering 5% ellipticity, the effective refractive index between the even and odd modes of almost all orders rises to $\Delta n_{\rm off} \approx 10^{-7}$. The walk-off length is just tens of meters. Thus, in reality, OAM modes generated by combining the even and odd modes are unstable in propagation, too. To avoid this effect, the OAM transfer fibers should be carefully designed to make the $\Delta n_{\rm eff}$ smaller and should be protected well from external perturbations.

4 Conclusion

We have constructed a four-dimensional complex space model and derived the complete transformation relation connecting arbitrary Ith order CV modes and OAM modes in fiber systems. No matter what the desired OAM modes in fibers are, there must be a specific group of intrinsic CV modes corresponding with them and that can be calculated. The results in previous articles and ours verify the reliability of the constructed complex space model. Using this model, we succeeded in explaining many results reported in previous articles and extended these results into more general situations. That is, we predicted the existence of elliptical polarized OAM modes in fibers, which are the most general states and have not been discussed before.

Besides generating a single pure OAM mode from the combination of CV modes, there are some other states that can be utilized. That is, if a hybrid state consists of two orthogonal polarized OAM modes with opposite TCs, we can obtain the two pure OAM modes, respectively, by a QWP and a polarizer (or a birefringent crystal) with a particular angle. Compared with the states generating a single pure OAM mode directly, the TC is tunable in these states. We also researched on these states and gave the simulation and experiment results.

Then, we analyzed the effect of different propagation constants. When OAM modes are generated by several CV modes with different propagation constants, the TCs of the OAM modes change periodically along with the transmission distance. To avoid this effect, the OAM transfer fibers should be carefully designed and protected to make the difference in propagation constants between the four degenerated CV modes smaller.

In summary, we demonstrated the complete transformation relation connecting arbitrary lth order CV modes and OAM modes. Also, we verified some common situations and gave the general formulas to describe the corresponding relations. These general formulas can explain previous articles well and include many results that have been reported in fiber OAM generation systems. This analysis method is able to describe arbitrary fields in fiber conveniently, which may have great potentials in the generation and application of arbitrary fields based on optical fibers.

Acknowledgments: This work was jointly supported by the National Natural Science Foundation of China under Grant Nos. 11674177, 61775107, 11704283 and 61835006, Tianjin Natural Science Foundation under Grant No. 16JCZDJC31000, the National Key Research and Development Program of China under Grant Nos. 2018YFB0504401 and 2018YFB070, and the 111 Project (B16027).

References

- [1] Zhan QW. Cylindrical vector beams: from mathematical concepts to applications. Adv Opt Photonics 2009;1:1-57.
- [2] Kozawa Y, Sato S. Optical trapping of micrometer-sized dielectric particles by cylindrical vector beams. Opt Express 2010;18:10828-33.
- [3] Min CJ, Shen Z, Shen JF, et al. Focused plasmonic trapping of metallic particles. Nat Commun 2013;4:2891.
- [4] Xie XS, Chen YZ, Yang K, Zhou JY. Harnessing the point-spread function for high-resolution far-field optical microscopy. Phys Rev Lett 2014;113:263901.
- [5] Salakhutdinov V, Sondermann M, Carbone L, Giacobino E, Bramati A, Leuchs G. Optical trapping of nanoparticles by full solid-angle focusing. Optica 2016;3:1181-6.
- [6] Chen R, Agarwal K, Sheppard CJR, Chen XD. Imaging using cylindrical vector beams in a high-numerical-aperture microscopy system. Opt Lett 2013;38:3111-4.
- [7] D'Ambrosio V, Nagali E, Walborn SP, et al. Complete experimental toolbox for alignment-free quantum communication. Nat Commun 2012;3:961.
- [8] Vallone G, D'Ambrosio V, Sponselli A, et al. Free-space quantum key distribution by rotation-invariant twisted photons. Phys Rev Lett 2014;113:060503.
- [9] Milione G, Nguyen TA, Leach J, Nolan DA, Alfano RR. Using the nonseparability of vector beams to encode information for optical communication. Opt Lett 2015;40:4887-90.
- [10] Zhao YF, Wang J. High-base vector beam encoding/decoding for visible-light communications. Opt Lett 2015;40:4843-6.
- [11] Kruk S, Ferreira F, Mac Suibhne N, et al. Transparent dielectric metasurfaces for spatial mode multiplexing. Laser Photonics Rev 2018;12:1800031.
- [12] Parigi V, D'Ambrosio V, Arnold C, Marrucci L, Sciarrino F, Laurat J. Storage and retrieval of vector beams of light in a multiple-degree-of-freedom quantum memory. Nat Commun 2015;6:7706.
- [13] Allen L, Beijersbergen MW, Spreeuw RJC, Woerdman JP. Orbital angular momentum of light and the transformation of Laguerre-Gaussian laser modes. Phys Rev A Atom Mol Opt Phys 1992;45:8185.
- [14] Yao AM, Padgett MJ. Orbital angular momentum: origins, behavior and applications. Adv Opt Photonics 2011;3:161-204.
- [15] Ramachandran S, Kristensen P. Optical vortices in fiber. Nanophotonics-Berlin 2013;2:455-74.
- [16] Forbes A, Dudley A, McLaren M. Creation and detection of optical modes with spatial light modulators. Adv Opt Photonics 2016:8:200-27.
- [17] Padgett MJ. Orbital angular momentum 25 years on [Invited]. Opt Express 2017;25:11265-74.
- [18] Dholakia K, Cizmar T. Shaping the future of manipulation. Nat Photonics 2011;5:335-42.

- [19] Tkachenko G, Brasselet E. Helicity-dependent three-dimensional optical trapping of chiral microparticles. Nat Commun 2014;5:4491.
- [20] Paez-Lopez R, Ruiz U, Arrizon V, Ramos-Garcia R. Optical manipulation using optimal annular vortices. Opt Lett 2016;41:4138-41.
- [21] Furhapter S, Jesacher A, Bernet S, Ritsch-Marte M. Spiral interferometry. Opt Lett 2005;30:1953-5.
- [22] Curtis JE, Koss BA, Grier DG. Dynamic holographic optical tweezers. Opt Commun 2002:207:169-75.
- [23] Curtis JE, Grier DG. Modulated optical vortices. Opt Lett 2003:28:872-4.
- [24] Padgett M, Bowman R. Tweezers with a twist. Nat Photonics 2011;5:343-8.
- [25] Wang J, Yang JY, Fazal IM, et al. Terabit free-space data transmission employing orbital angular momentum multiplexing. Nat Photonics 2012;6:488-96.
- [26] Yan Y, Xie GD, Lavery MPJ, et al. High-capacity millimetre-wave communications with orbital angular momentum multiplexing. Nat Commun 2014;5:4876.
- [27] Huang H, Milione G, Lavery MPJ, et al. Mode division multiplexing using an orbital angular momentum mode sorter and MIMO-DSP over a graded-index few-mode optical fibre. Sci Rep-Uk 2015;5:14931.
- [28] Willner AE, Huang H, Yan Y, et al. Optical communications using orbital angular momentum beams, Adv Opt Photonics 2015;7:66-106.
- [29] Wang J. Advances in communications using optical vortices. Photonics Res 2016;4:B14-28.
- [30] Li Z, Liu W, Li Z, et al. Tripling the capacity of optical vortices by nonlinear metasurface. Laser Photonics Rev 2018;0:1800164.
- [31] Yang TS, Zhou ZQ, Hua YL, et al. Multiplexed storage and real-time manipulation based on a multiple degree-of-freedom quantum memory. Nat Commun 2018;9:3407.
- [32] Han Y, Liu YG, Wang Z, et al. Controllable all-fiber generation/ conversion of circularly polarized orbital angular momentum beams using long period fiber gratings. Nanophotonics-Berlin 2018;7:287-93.
- [33] Jiang YC, Ren GB, Lian YD, Zhu BF, Jin WX, Jian SS. Tunable orbital angular momentum generation in optical fibers. Opt Lett 2016;41:3535-8.
- [34] Jiang YC, Ren GB, Shen Y, et al. Two-dimensional tunable orbital angular momentum generation using a vortex fiber. Opt Lett 2017;42:5014-7.
- [35] Han Y, Chen L, Liu YG, et al. Orbital angular momentum transition of light using a cylindrical vector beam. Opt Lett 2018;43:2146-9.
- [36] Krishna CH, Roy S. Analyzing characteristics of spiral vector beams generated by mixing of orthogonal LP11 modes in a fewmode optical fiber. Appl Opt 2018;57:3853-8.
- [37] Wu H, Gao SC, Huang BS, et al. All-fiber second-order optical vortex generation based on strong modulated long-period grating in a four-mode fiber. Opt Lett 2017;42:5210-3.
- [38] Bozinovic N, Golowich S, Kristensen P, Ramachandran S. Control of orbital angular momentum of light with optical fibers. Opt Lett 2012;37:2451-3.
- [39] Wang L, Vaity P, Ung B, Messaddeq Y, Rusch LA, LaRochelle S. Characterization of OAM fibers using fiber Bragg gratings. Opt. Express 2014;22:15653-61.

- [40] Li SH, Mo Q, Hu X, Du C, Wang J. Controllable all-fiber orbital angular momentum mode converter. Opt Lett 2015;40:4376-9.
- [41] Jiang YC, Ren G, Jin WX, Xu Y, Jian W, Jian SS. Polarization properties of fiber-based orbital angular momentum modes. Opt Fiber Technol 2017;38:113-8.
- [42] Jiang YC, Ren GB, Li HS, et al. Tunable orbital angular momentum generation based on two orthogonal LP modes in optical fibers. IEEE Photonic Tech L 2017;29:901-4.
- [43] Zhang Y, Pang FF, Liu HH, et al. Generation of the first-order OAM modes in ring fibers by exerting pressure technology. IEEE Photonics J 2017;9:1-9.
- [44] Wu SH, Li Y, Feng LP, et al. Continuously tunable orbital angular momentum generation controlled by input linear polarization. Opt Lett 2018;43:2130-3.
- [45] Yao SZ, Ren GB, Shen Y, Jiang YC, Zhu BF, Jian SS. Tunable orbital angular momentum generation using all-fiber fused coupler. IEEE Photonic Tech L 2018;30:99-102.

- [46] Zhang XQ, Wang AT, Chen RS, Zhou Y, Ming H, Zhan QW. Generation and conversion of higher order optical vortices in optical fiber with helical fiber Bragg gratings. J Lightwave Technol 2016:34:2413-8.
- [47] Zhao YH, Liu YQ, Zhang CY, et al. All-fiber mode converter based on long-period fiber gratings written in few-mode fiber. Opt Lett 2017;42:4708-11.
- [48] Pidishety S, Pachava S, Gregg P, Ramachandran S, Brambilla G, Srinivasan B. Orbital angular momentum beam excitation using an all-fiber weakly fused mode selective coupler. Opt Lett 2017;42:4347-50.
- [49] Heng X, Gan J, Zhang Z, et al. All-fiber stable orbital angular momentum beam generation and propagation. Opt. Express 2018;26:17429.
- [50] Chen S, Wang J. Theoretical analyses on orbital angular momentum modes in conventional graded-index multimode fibre. Sci Rep-Uk 2017;7:3990.